

# Effect of connectivity and wettability on the relative permeability of NAPLs

Liang-Cheng Chang · Hung-Hui Chen ·  
Hsin-Yu Shan · Jui-Pin Tsai

Received: 27 January 2008 / Accepted: 4 February 2008 / Published online: 26 February 2008  
© Springer-Verlag 2008

**Abstract** The characteristic relationships among relative permeability ( $K_r$ ), saturation ( $S$ ) and capillary pressure ( $P$ ) of NAPLs are the important constitutive laws to simulate the NAPLs flow in the subsurface. In this study, a micro model was used to obtain the values of permeability, saturation for the multi-phase flow of five fluid-pairs. The perspective micro model allows one to clearly observe the multiphase flow and allow this study to precisely measure the fluid saturation by digital image analysis. The experimental results showed hysteresis phenomenon of relative permeability versus saturation and that was not interpreted by previous studies. By carefully examining the recorded images, this study found that the degree of the connectivity for the micro channel occupied by wetting phase fluid could influence the relative permeability. Therefore, for the same saturation, the relative permeability in the imbibition is higher than that in the drainage. The results of the  $K_r$ - $S$  experiments for five fluid-pairs also showed that the residual saturation of wetting phase fluid decreased with the wettability increasing but increased with the interfacial tension increasing. Those interpretations and experimental

results are valuable references for groundwater remediation and oil reservoir development.

**Keywords** NAPLs · Relative permeability · Micro model · Imbibition · Connectivity · Micro channel

## Introduction

The contamination of groundwater by organic solvents, such as trichloroethylene (TCE), tetrachloroethylene (PCE) and other petroleum-based products has raised considerable concerns because of its serious threat to human health. Most of these organic solvents are liquid phases in the subsurface with low solubility in water and are called non-aqueous phase liquids (NAPLs). These NAPLs or their solutions, even at low concentrations, can have severely adverse effects on human health over the long-term. Consequently, they will seriously threaten the environment if toxic NAPLs penetrate into groundwater accidentally (Das et al. 2006). During their downward movements, some of the NAPLs will remain in the pore spaces of soil, and are known as residuals. These residuals are discontinuous and their movements are difficult to predict. The density of the NAPLs has a decisive influence on their flow behaviors. Therefore, the NAPLs are grouped into two classes: (1) LNAPLs (light NAPLs) which are lighter than water and float on top of the water table; (2) DNAPLs (dense NAPLs) which are denser than water and can penetrate the water table moving deeper into the aquifer system (Bedient et al. 1994).

The two-phase flow behavior in the subsurface is a very complex process and is governed by a number of material-dependent parameters and the relationships between relative permeability ( $K_r$ ), saturation ( $S$ ) and capillary pressure

---

L.-C. Chang (✉) · H.-H. Chen · H.-Y. Shan · J.-P. Tsai  
Department of the Civil Engineering,  
National Chiao Tung University, Hsin Chu, Taiwan  
e-mail: lcchang@chang.cv.nctu.edu.tw

H.-Y. Shan  
e-mail: hyshan@mail.nctu.edu.tw

J.-P. Tsai  
e-mail: scorpio@chang.cv.nctu.edu.tw

H.-H. Chen  
Department of the Civil Engineering,  
Min Hsin University Science Technology, Hsin Chu, Taiwan  
e-mail: chf@chang.cv.nctu.edu.tw

( $P$ ). In general, the lack of experimental information on constitutive relations may be the foremost element impeding the development of modeling to accurately predict and assess environmental consequences of subsurface NAPL contamination (Helmig 1997; Oostrom and Lenhard 1998).

The efforts to characterize the behaviors of NAPLs in the subsurface include field investigation at contaminated sites, sand tank experiments, and computer simulations. Among these approaches, examining NAPL spills on field sites were arduous, expensive and most likely, imprecise processes (Demond et al. 1993). The sand tank model was conventionally adopted to examine the relation between permeability and saturation and was used to study the fluid flow and distribution for a NAPL spill. However, the model was difficult to control, had a low accuracy, and lacked experimental repeatability (Soll et al. 1993). Because of the opaque of porous media, the sand tank model is difficult to observe the flow of NAPLs during the experiment. By solving sets of governing equations, numerical models were used to estimate the volumes and distribution of contaminants under the assumed conditions. However, to perform a numerical simulation, the relations among the relative permeability ( $K_r$ ), saturation ( $S$ ), and capillary pressure ( $P$ ) of NAPLs required to be given and that played a pivotal role in simulating the fate and flow process of NAPLs in porous media.

The  $P$ – $S$  relationships quantify the level of saturation (water content or level of fluid hold up by volume) as a function of capillary pressure in porous media. On the other hand, the  $K_r$ – $S$  relationships quantify the relative permeability of the porous domain to a particular fluid phase (e.g., NAPL) at different fluid saturation values. The effects of all fluids and material properties are then lumped into the nonlinear  $K_r$ – $S$ – $P$  curves for multiphase flow in a porous domain. Two-phase flow experiments on soils with different properties (e.g., particle and pore size distribution, permeability, etc.) result in different  $K_r$ – $S$ – $P$  curves. These cause non-uniqueness in the  $K_r$ – $S$ – $P$  curves.

$K_r$ – $S$ – $P$  relationships were influenced by the interplay of a number of other factors, e.g., initial water saturation in the domain; wettability of the solid grains to particular fluid phase; contact angles between the fluid phases and solid grains; pore and particle size distribution; fluid properties (e.g., viscosity, density); interfacial tension; gravity forces; types of heterogeneities; domains size; hysteresis, etc. (Baker 1988; Hassanizadeh et al. 2002a, b; Theodoropoulou et al. 2003; Das et al. 2004; Hilfer 2006). Because of a complex interplay between these factors, it is generally not possible to measure unique  $K_r$ – $S$ – $P$  relationships for a porous sample. This introduces difficulties in using the measured  $K_r$ – $S$ – $P$  relationships to practical problems. In past 10 years, attempts have been made to improve the

predictability of multi-phase flow models by developing various types of theories and scaling rules (Busby et al. 1995; Bradford et al. 1996; Ataie-Ashtiani et al. 2001). Therefore, there have been a number of attempts to characterize how the variations in the above factors cause non-uniqueness in these relationships in an attempt to generalize their effects as far as possible (Ataie-Ashtiani et al. 2002, 2003; Das et al. 2004). Fagerlund et al. (2006) compared the performance of applying different  $K_r$ – $S$ – $P$  model on simulating the NAPL migration. Their work showed that with the inclusion of a nonlinear NAPL tortuosity factor, both the Brooks–Corey–Burdine and van Genuchten–Mualem models yielded excellent fits to experimental data. Li et al. (2004) developed a scaling model to scale the spontaneous imbibition data that could consider with relative permeability, capillary pressure, wettability and gravity. Li (2007) further extend to develop the scaling model to consider the wettability. On the other hand, van Dijke et al. (2002) had proposed a model about the relation between interfacial tensions and wettability in three-phase systems, consequences for pore occupancy and relative permeability. Moreover, they recommend that experiments must be performed to identify these quantities.

Transparent micro models were emerged as a promising experimental tool. The main idea of micro models was to represent the structure of the porous medium using an interconnected pore network (Soll 1993). They had investigated the physical processes involved in a three-phase system used micro model. Facilitating by digital image analysis, they obtained three-phase, water, oil and air, capillary pressure–saturation ( $P$ – $S$ ) relationships at pore-scale. Jeong et al. (2000) individually had performed experimental studies on the miscible displacement (i.e., solute flow) in micro models. Corapcioglu et al. (1997, 1999) used etched micro models with specified geometry and topology to observe the trapping mechanism during NAPL movement. Jia et al. (1999) had employed image-analyzing techniques to quantify the miscible displacement and solute transport in an etched glass micro model and compared the experimental data with numerical model results.

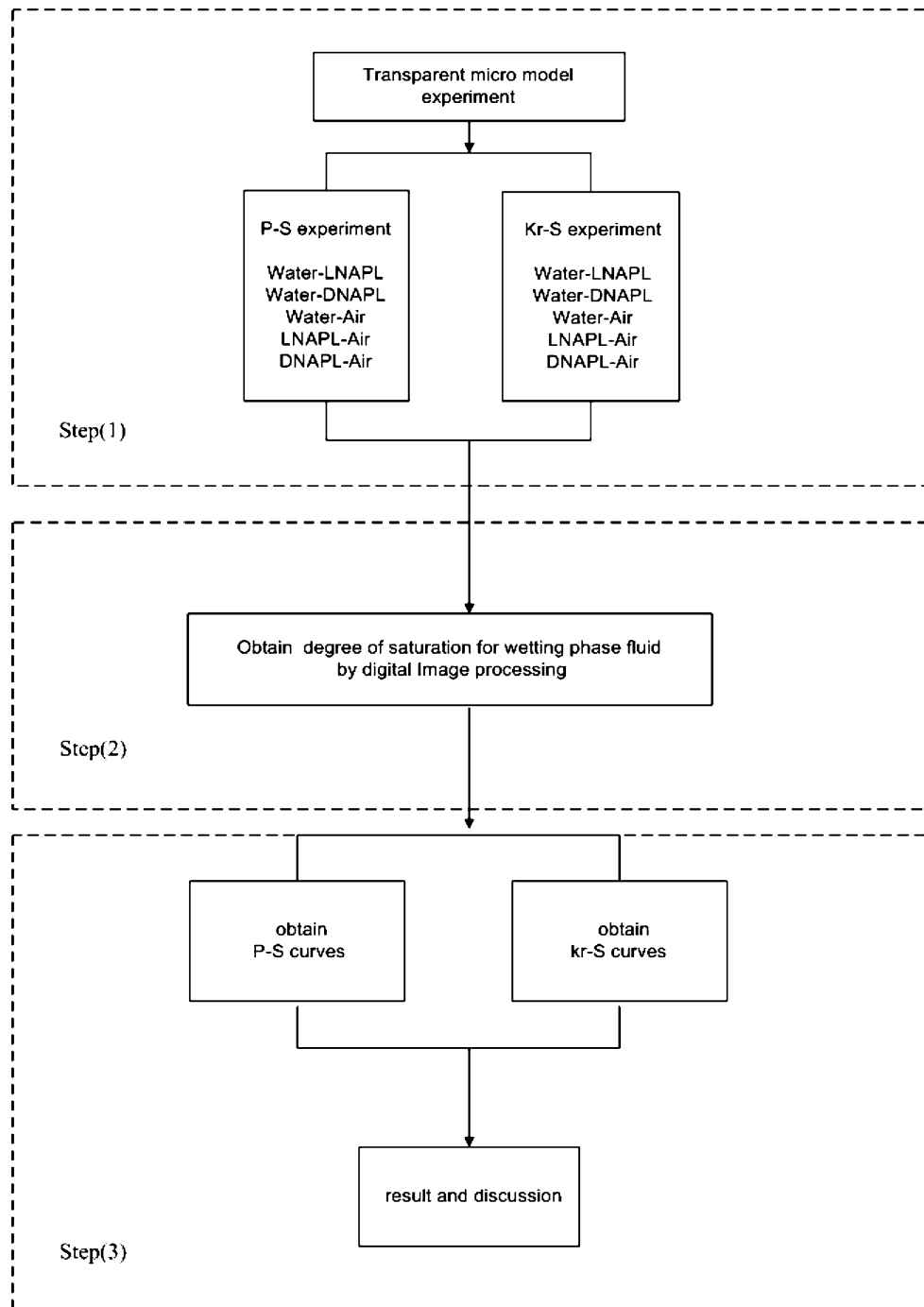
Al-Futaisi et al. (2004) had investigated the spontaneous and forced secondary imbibition of NAPL-invaded sediment using a pore network model. They had used a single network geometry and connectivity, but with three different levels of mixed-wetting: water-wet, intermediate-wet, and NAPL-wet. They simulated secondary imbibition (water displacing NAPL) and conducted a parametric study of imbibition by varying systematically the controlling parameters: the advancing contact angles, the fraction of NAPL-wet pores, the interfacial tension, and the initial water saturation. They indicated that the range of advancing contact angles and the fraction of NAPL-wet pores had

dramatic effects on the NAPL-water capillary pressures and relative permeability. The spatially inhomogeneous interfacial tension had a minor impact on the trapped NAPL saturation and relative permeability to NAPL, and a slight effect on the relative permeability to water.

As so far, few micro model studies have been performed on the degree of the connectivity for the micro channel (pores and throats) occupied by wetting phase fluid can influence the relative permeability. Therefore, this study used a micro model to obtain the values of

relative permeability, saturation for the multi-phase fluid flow. The perspective micro models allowed us to clearly observe the multiphase flow systems and allowed this study precisely to measure the saturation of media (micro model) by digital image analysis. This paper focused on studying how the degree of the connectivity for the micro channel (pores and throats) occupied by wetting phase fluid could influence the relative permeability when using micro model. Figure 1 shows the overall research procedure of this study.

**Fig. 1** Research procedure



## Related theory

### Young–Laplace equation

The Young–Laplace equation was used to describe the relation among the capillary pressure, interfacial tension and meniscus curvature for a fluid pair in a single tube (Leverett et al. 1942; Parker et al. 1987; van Dijke et al. 2007) and was written as Eq 1.

$$P_{ij} = \frac{2\sigma_{ij}}{R_{ij}} \quad (1)$$

where  $P_{ij} = P_i - P_j$  denotes the pressure difference between the phases;  $\sigma_{ij}$  is the interfacial tension and  $R_{ij}$  is the radius of curvature of the meniscus between  $i$  phase fluid and  $j$  phase fluid, respectively. For a tube, the  $P_{ij}$  reaches a critical value ( $P_c$ ) when the  $R_{ij}$  equals to the tube radius. The meniscus will collapse and non-wetting fluid will occupy the tube if the capillary pressure is greater than the critical value. The critical capillary was also known as capillary entry pressure (Lenormand et al. 1983; Legait et al. 1983; Dullien 1992).

### Darcy's law

Darcy's law is one of the basic relationships to describe the fluid flow in porous media and it is extended to multiphase flow with permeability replaced by phase permeability. This approximation is a valid and reasonable model if the interfaces between the fluids remain static. The definition of relative permeability is derived from the extension of Darcy's law to multi-phase flow (Muskat et al. 1936; Wessolek et al. 1994). Assuming that the flow of a phase in the presence of the other phase can be viewed as single phase flow through a reduced pore network, the subscript  $i$  can be added for each phase to Darcy's law as:

$$q_i = -[k_i(S)/\mu_i](\nabla P_i - \rho_i g \nabla Z_i) \quad (2)$$

where  $q_i$  is flow of a fluid phase per unit total area perpendicular to the flow, or specific discharge,  $k_i(S)$  is effective permeability as a function of saturation,  $\mu$  is fluid viscosity,  $P_i$  is pressure of the  $i$ th phase liquid,  $\rho$  is density,  $g$  is gravitational acceleration constant,  $Z_i$  is elevation above a datum,  $i$  is  $i$ th phase,  $S$  is the saturation level for  $i$ th phase fluid,  $k_i(S)/\mu_i$  is the unsaturated conductivity for  $i$ th phase fluid.

A relative permeability to a particular fluid is usually defined as the ratio of the effective permeability to that fluid to intrinsic permeability of the porous media. For a specific fluid,

$$k_{ri}(S) = k_i(S)/k = K_i(S)/K_i \quad (3)$$

where  $K_{ri}(S)$  is the relative permeability of the  $i$ th phase fluid;  $K$  is the intrinsic permeability,  $K_i$  is the saturated conductivity of the  $i$ th phase fluid.

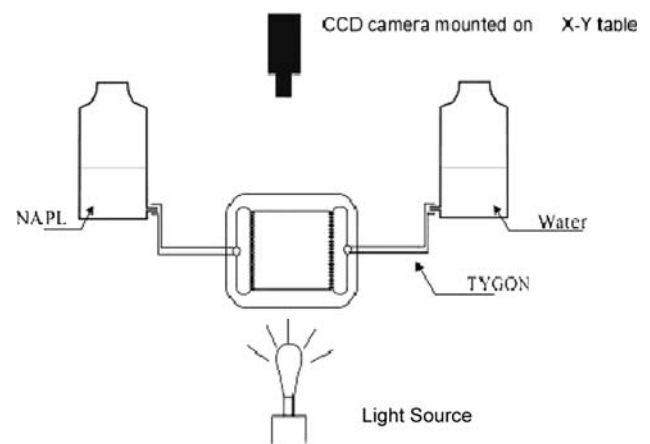
## Research procedure

Figure 1 shows the overall research procedure of this study. In Fig. 1, step 1 indicates that various micro model experiments of  $P$ – $S$  and  $K_r$ – $S$  associated to different fluids pairs were performed. Step 2 indicates using digital image analysis to obtain the degree of saturation from the image recorded in step 1. Step 3 shows the result and discussion of the experimental  $P$ – $S$  and  $K_r$ – $S$  values.

## Experimental design

### Experiment system

The experimental system for  $P$ – $S$  experiments (see Fig. 2) was consisted of a transparent acrylic micro model, head control sub-system, CCD camera and light source. The head control sub-system included connecting tubes and glass containers (reservoirs) and their elevations could be freely adjusted to control the heads. The two sides of the micro model were connected to inflow and outflow reservoirs, respectively. Images of the whole micro model were taken from the CCD camera to record fluids distribution during the experiment. The  $P$ – $S$  experiment is basically a static experiment. The fluids were static at the end of each stage of the experiment while the degree of saturation for each phase varied according to the capillary pressure. On the other hand, the  $K_r$ – $S$  experiments needed to maintain a fluid flow with constant velocity, and that required the system to maintain a constant gradient. Figure 3 was the



**Fig. 2** Schematic diagram of the experimental system for  $P$ – $S$  experiments

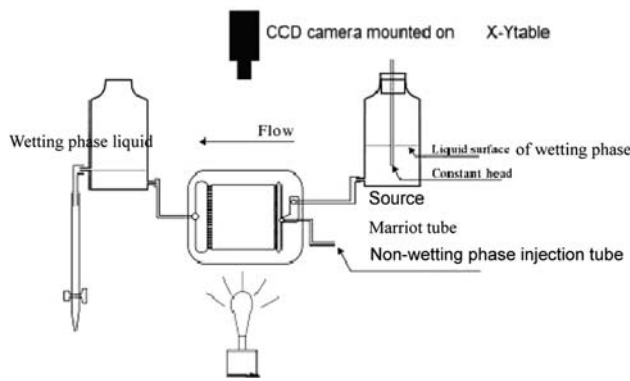


**Fig. 3** Schematic diagram of the experimental system for  $K_r$ - $S$  experiments

experimental system for  $K_r$ - $S$  experiments and it showed several important differences to the  $P$ - $S$  system. Those are: (1) Marriot tube and glass container with overflow tube were applied to maintain a constant head difference between inflow and outflow boundary of the micro model. The constant head of the Marriot Tube was higher than that of the glass container during the experiments; (2) a non-wetting injection tube to inject the non-wetting phase liquid during the experiments was added. The injection of non-wetting phase liquid could vary the degree of saturation for both wetting and non-wetting phase in the micro model.

**Micro model**

Micro model is the most important component of the experimental system. Figure 4 shows the schematic diagram of micro model for  $P$ - $S$  experiments and Fig. 5 is that of micro model for  $K_r$ - $S$  experiments. Both micro models consist of 400 pores and 760 throats. The pores and throats are connected to each other with a grid pattern as shown. The distance between the centers of two adjacent pores was 2.2 mm. For each pores and throats, the widths were

selected randomly from five predetermined sizes using Visual Basic Application (VBA) in AUTOCAD. Table 1 lists the widths and numbers of the pores and throats obtained in this study. In Table 1, the equivalent radius of the pores and throats were calculated according to geometric relation with following Eq 4 (Lenormand 1983; Legait and Jacquin 1983).

$$\frac{1}{R} = \frac{1}{w} + \frac{1}{d} \tag{4}$$

where  $R$  is the equivalent radius of the pores or throats,  $w$  is the width of pores or throats and  $d$  is the depth. The depth of all pores and throats in the micro model is designed the same as 0.8 mm. Table 1 showed the equivalent radius of the pores and throats for the micro model. According to Eq 1, the equivalent radius and interfacial tension define the critical capillary pressure. Therefore, for a specific fluid pair, each pore or throat within the micro model has critical capillary pressure, respectively. When the capillary pressure is less than the minimal critical capillary pressure, the micro model will fill with wetting phase fluid. On the other hand, the micro model will fill with non-wetting phase fluid when the capillary pressure is greater than the maximum critical capillary pressure. Therefore, the situation limited the feasible range of capillary pressure for the experiment. Since each fluid pair has its own interfacial tension respectively, the feasible experimental range of capillary pressure will vary for each fluid pairs. For the micro model with the pores and throats structure as shown in Table 1; Table 2 showed the experimental range of capillary pressure of the five fluid pairs: water–air, diesel fuel–air, Pca–air, water–diesel fuel, and water–Pca. The contact angle  $\theta$  is assumed to be zero in each fluid-pair.

For both  $P$ - $S$  and  $K_r$ - $S$  micro model, barriers were required to confine the non-wetting fluid in the micro model during experiment. The barriers consisted of many

**Fig. 4** Schematic diagram of micro-model for  $P$ - $S$  curves

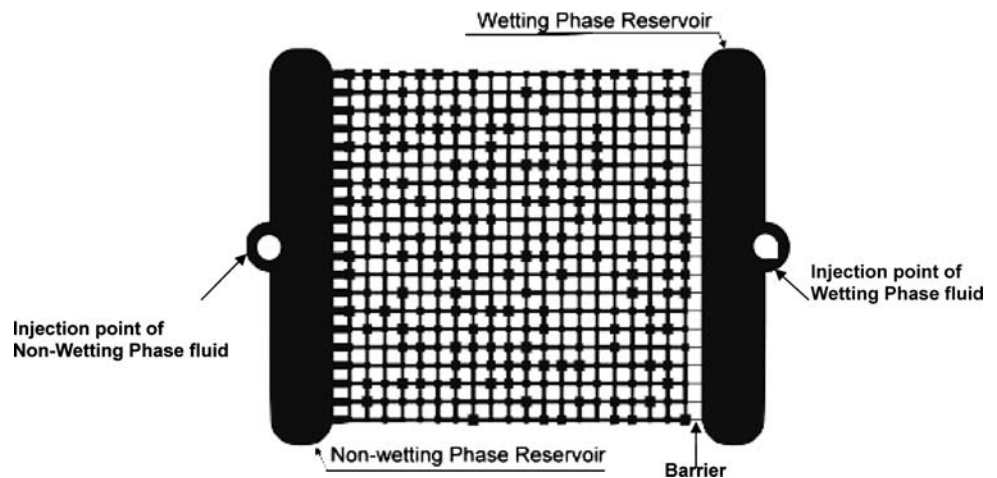




**Fig. 5** Schematic diagram of micro-model for  $K_r$ - $S$  curves

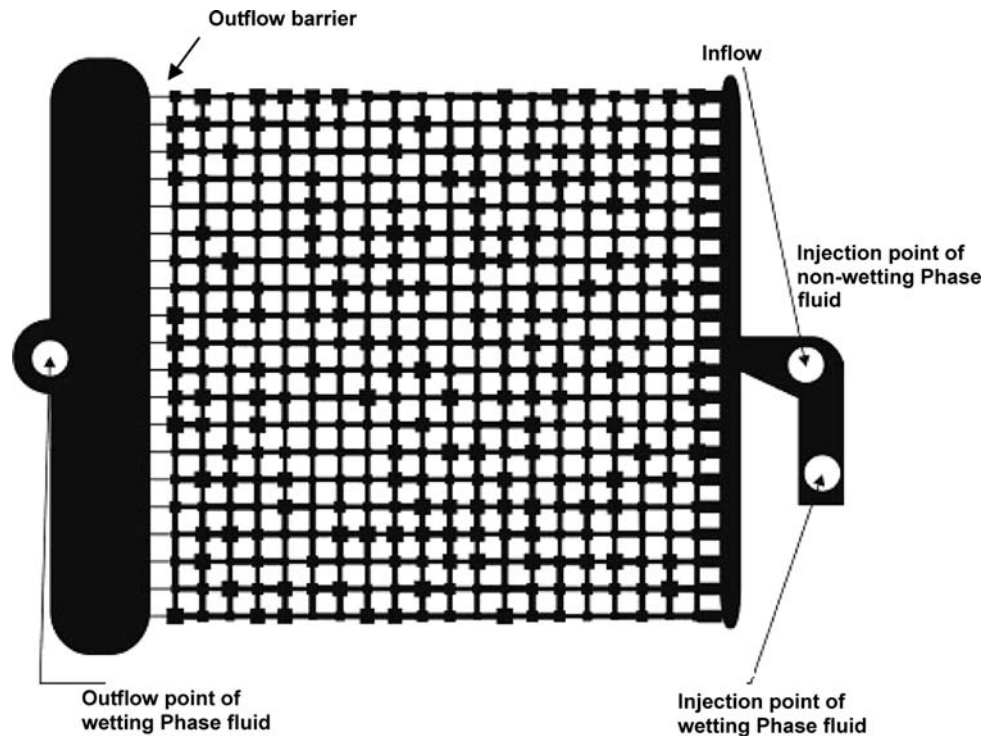


**Table 1** The sizes and numbers of the pores and throats in micro model

	Pore/throat width (mm)	Equivalent radius (mm)	Pore/throat numbers
Throat	0.3	0.218	160
	0.34	0.239	168
	0.38	0.258	142
	0.42	0.275	132
	0.46	0.292	158
Pore	0.6	0.343	64
	0.72	0.379	88
	0.88	0.419	98
	1.04	0.452	84
	1.28	0.492	66

parallel micro-channels. The narrow width of the micro-channel created a condition that the capillary pressure in the micro-channel must be greater than an 'entry pressure' for the non-wetting phase fluid to pass through the barrier. Therefore, the width of the micro-channels was smaller than the minimal width of the pores or throats in the micro model. Figure 4 shows that the barrier of  $P$ - $S$  micro model located at the boundary of the wetting phase fluid reservoir to prevent the non-wetting phase fluid leaking into the reservoir. Figure 5 indicates that the barrier of  $K_r$ - $S$  micro model was located in the outflow side of the micro model to prevent the non-wetting phase fluid flowing out of the micro model. The width of each micro-channel in the barrier is 0.1 mm for  $P$ - $S$  micro model and is 0.2 mm for

**Table 2** The interfacial tension and experimental ranges of capillary pressure for five fluid-pairs

Fluid pairs	Interfacial tension (dyne/cm)	Experimental ranges of capillary pressure (cm)
Water-air	71.5	2.97 ~ 6.70
Diesel fuel-air	22.8	0.95 ~ 2.14
Pca-air	32.75	1.36 ~ 3.07
Water-diesel fuel	48.7	2.02 ~ 4.56
Water-Pca	38.75	1.61 ~ 3.63

$K_r$ - $S$  micro model. The dark color of Figs. 4 and 5 shows the pores and throats with varied sizes in the micro model.

The acrylic surface is hydrophobic and is different to the wetting condition of the soil particle surface generally. Therefore, the micro model was coated by silicate to change its surface into hydrophilic. The surface of the micro model was coated with a thin film of silicate ( $\text{SiO}_2 \cdot n\text{Na}_2\text{O} \cdot x\text{H}_2\text{O}$ ,  $n = 2 \sim 4$ ) and was heated in the oven under  $110^\circ\text{C}$ . Figure 6 demonstrates that the silicate coating indeed changed the wetting characteristic of the micro model from hydrophobic (Fig. 6a) to hydrophilic (Fig. 6b).

#### CCD camera

The CCD camera was mounted on an  $x$ - $y$  table and above the micro model. The camera could move freely in three

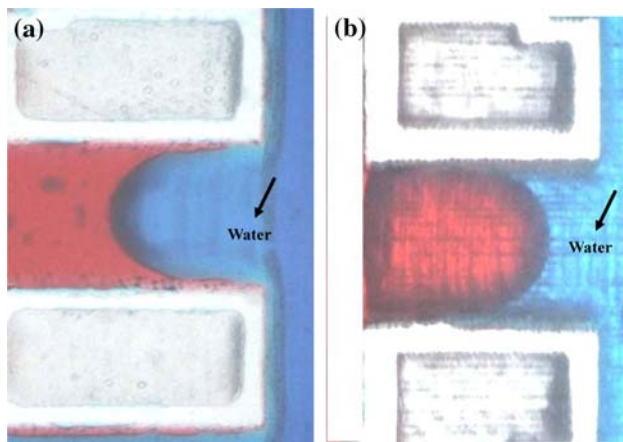


**Fig. 6** the surfaces of the pores and throats in micro model was coated with a thin Film of silicate ( $\text{SiO}_2 \cdot n\text{Na}_2\text{O} \cdot x\text{H}_2\text{O}$ ,  $n = 2 \sim 4$ )

dimensions. The images were recorded in digital signals and stored in the personal computer. The resolutions of the CCD are  $640 \times 480$  pixels and each pixel was represented as RGB format. During the experiment, images were taken by the CCD camera in a time interval of 30 s. The recorded RGB images were explored by PHOTOSHOP software to determine the degree of saturation for both wetting and non-wetting phase fluids.

**Experimental fluids**

Diesel fuel and tetrachloroethane (Pca) were chosen to represent the LNAPL and DNAPL, respectively. The experimental fluids are dyed with different color to enhance visual observations and facilitate the imagine analysis of their saturation in micro model. The de-ionized water was dyed blue and the diesel fuel was dyed red. Since the concentrations of the dyes in the liquids were less than 0.05%, the dyes could have least impact on the results of *P-S* and *Kr-S* experiments. The properties of the liquids are listed in Table 3.

This study examined five fluid pairs and those were water–air, diesel fuel–air, Pca–air, water–diesel fuel and water–Pca. The interfacial tension of each fluid pair is the difference of the surface tension between associated fluids.

**Table 3** Physical property of the test fluids

Experimental fluids	Density ( $\text{g}/\text{cm}^3$ ) (24°C)	Surface tension (dynes/cm)
Water	0.997	71.5
Diesel fuel	0.820	22.8
Tetrachloroethane (Pca)	1.600	32.7

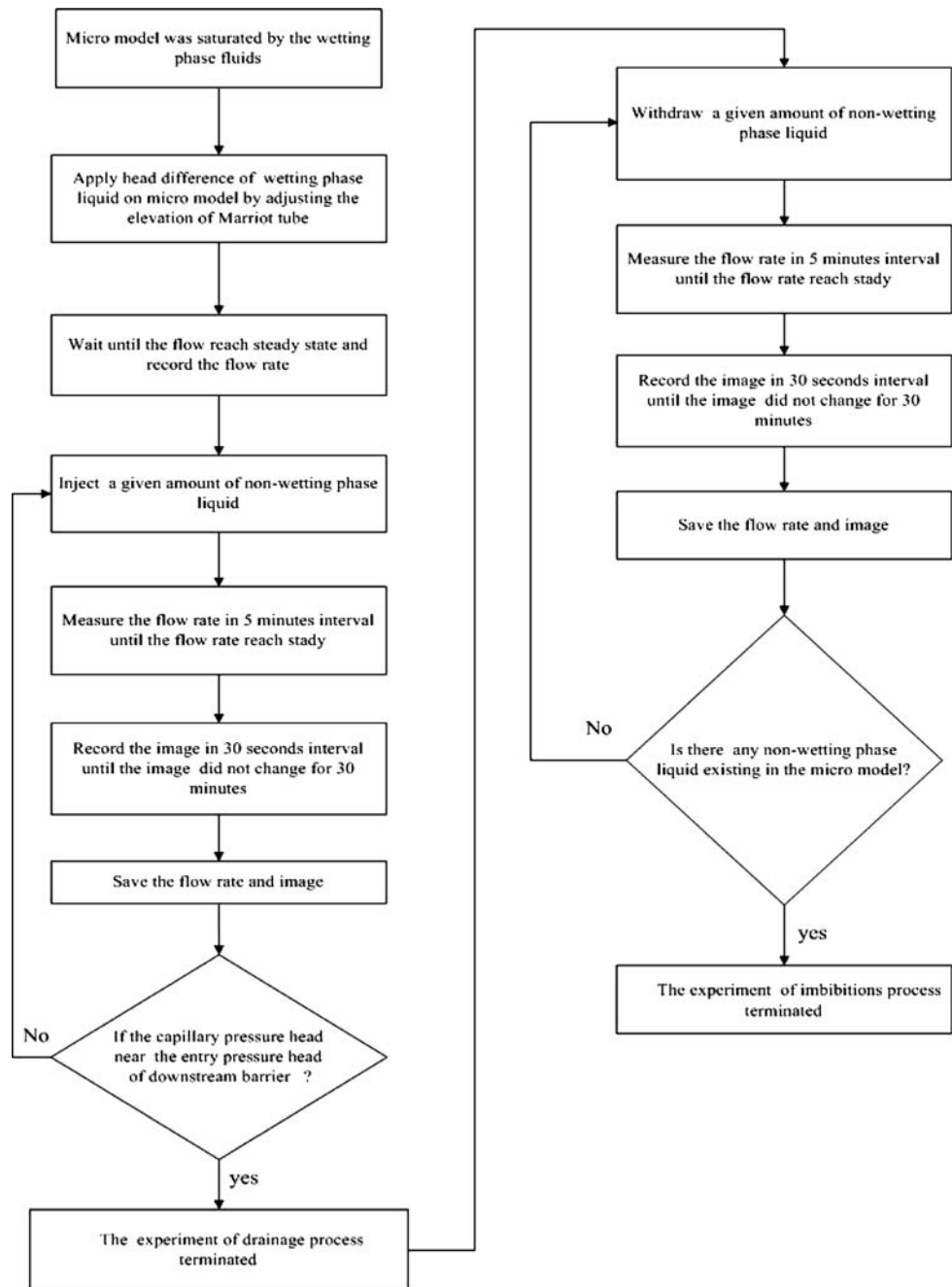
**Experiment procedure**

Figure 7 shows the experimental procedure of the *Kr-S* experiment. All the *Kr-S* experiments were conducted at 24°C. The experiment consisted of two main stages: the drainage process and imbibition process. The micro model was saturated with wetting phase fluids in the beginning. A constant head difference of the wetting phase was kept by adjusting the elevation of Marriot tube and then waited until the wetting phase flow reaches steady before starting the experiment. For the drainage process, the non-wetting liquid was injected into the micro model step by step through the injecting/withdrawing point shown in Fig. 5. In each step, the wetting phase flow rate was measured in a 5-min interval until its reaches steady state. The micro model images were taken by the CCD camera in a 30-s interval until the images did not change. The steady flow rate and the images were then recorded. The drainage process ended when the capillary pressure head neared the entry pressure head of the downstream barrier. For the imbibition process, the non-wetting phase fluid was withdrawn out of the micro model step by step through the same injecting/withdrawing point. At each step, the flow rate was measured and the images were taken similar to the drainage process. The imbibition process ended when there was nearly no more non-wetting fluid existed in the micro model. For both drainage and imbibition process, the conductivities  $K_i(S)$  of the micro model for the *i*th wetting phase liquid at different saturation level can be computed by the associated recorded flow rate ( $q_i$ ) and the constant head difference using the Darcy’s law (Eq 2). The relative permeability,  $K_{ri}(S)$ , defined by Eq 3 for a saturation level can be computed herein.

**Results and discussion**

Figures 8, 9, 10, 11, 12 showed the experimental *Kr-S* curves of the five fluid pairs and the results indicated that the relative permeability existed hysteresis phenomenon for all the fluid pairs. The permeability in the imbibition process was larger than those in the drainage process for the same wetting phase saturation. According to Eq 3 and other theoretical studies (van Dijke et al. 2001), the relative permeability is, in principle, expected to be function of saturation only. However, the experimental results of this study and other experimental researches (Kalaydjian et al. 1997) showed the existence of hysteresis phenomenon. The discrepancy can be explained by the pore scale connectivity of the wetting phase fluid in the micro model. Figure 13 showed the images of the fluids distribution in the micro model at selected experimental steps for the water–diesel fuel. According to Fig. 13, the non-wetting

**Fig. 7**  $Kr$ - $S$  experimental procedure



phase liquids (diesel fuel) were distributed more uniformly in the imbibition process (Fig. 13a, b) than that in drainage (Fig. 13a, b) for the similar wetting phase saturation. This implied that the connectivity of the wetting phases in the imbibition process (Fig. 13a, b) were better than that in the drainage process (Fig. 13a, b). Therefore, the relative permeability in the imbibition process was larger than that in the drainage process for the same wetting phase saturation. Similar results had been observed in previous studies (Kalaydjian 1997). Besides, by comparing the results shown in the Figs. 14 and 15, the relative permeability is approximately a linear function of the saturation

during the imbibition process, but the functional relation of relative permeability versus saturation is nonlinear in the drainage process. This phenomenon can be explored qualitatively. Because of the well connectivity in the imbibition process, the relative permeability of the wetting phase was expected to be function of the numbers of pore and throat occupied by the wetting phase fluid in the micro model. Since the occupied pore and throat numbers are linear function of the saturation, the relative permeability is also expected to be linear function of that.

Figure 14 shows the experimental  $Kr$ - $S$  values in drainage process for all the five fluid-pairs. All the drainage



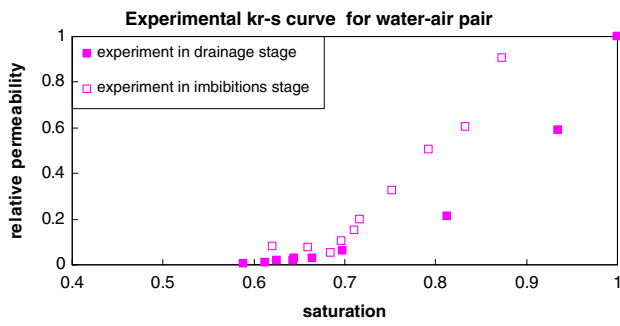


Fig. 8 The experimental  $K_r$ - $S$  curves of the water–air pair

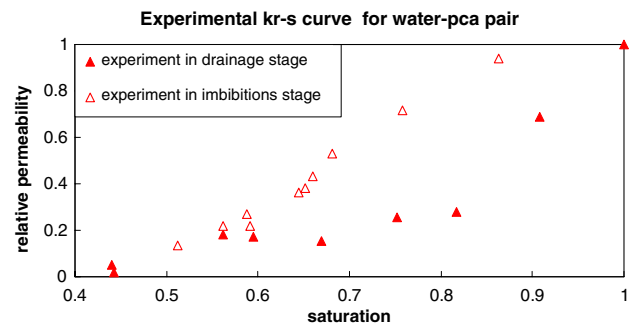


Fig. 12 The experimental  $K_r$ - $S$  curves of water–Pca pair

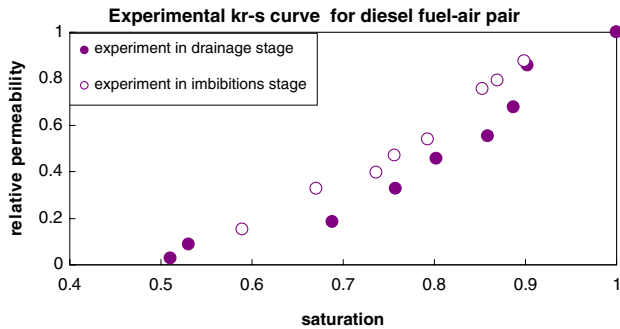


Fig. 9 The experimental  $K_r$ - $S$  curves of diesel fuel–air pair

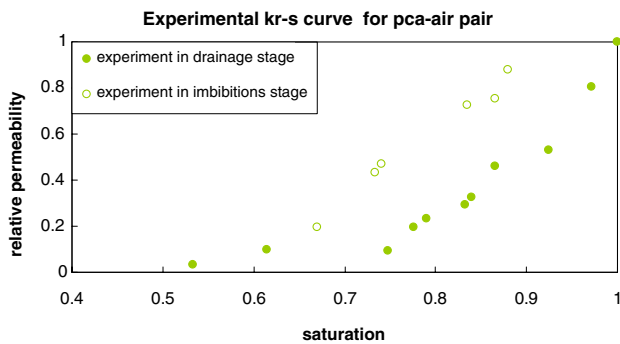


Fig. 10 The experimental  $K_r$ - $S$  curves of Pca–air pair

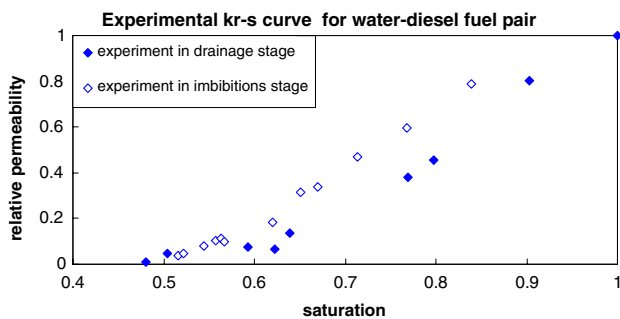


Fig. 11 The experimental  $K_r$ - $S$  curves of water–diesel fuel pair

curves are very similar and can be represented approximately with single drainage curve. However, if examining Fig. 14 more closely, the minimum wetting fluid saturations

(residual saturation) of the five fluid-pairs are different for relative permeability approaching zero. According to the experimental procedure (Fig. 7), the residual saturation occurs at the end of drainage process that is also the beginning of imbibition process. The wetting fluid residual saturation is the minimum saturation that the wetting fluid can still maintain the flow in the micro model. On the other hand, the ‘easier’ the wetting phase fluid move the smaller residual saturation of the wetting fluid. The wettability and interfacial tension factors are two factors influencing the residual saturation. In principle, a wetting fluid with higher wettability can maintain the corner flow at a smaller saturation, therefore, the fluid stops flowing (the relative permeability approaching zero) at a smaller saturation. On the contrary, the interfacial tension on the surface of two immiscible fluids creates a resistance on the flow. Hence, a fluid-pair with lower interfacial tension can have smaller wetting residual saturation. To summary, the wetting fluid’s residual saturation decreases with the wettability increasing but increases with the interfacial tension increasing. As shown in Table 4, the wetting residual saturations for the fluid pairs are water–Pca; water–diesel, diesel–air, Pca–air, and water–air in ascend. According to previous discussion, the residual saturations for the fluid-pairs that include water as wetting phase should be smaller than that of other fluid-pairs, and that is true for the water–Pca and water–diesel but not the water–air. The high residual saturation of the water–air can be explained by its large interfacial tension that is about 1.5–3 times of other fluid-pairs indicated in Table 3. Hence, excepting the water–air pair, the residual saturations for other four fluid-pairs can be divided into two groups; those with water and others without water, and the residual saturation increasing with the interfacial tension within each group.

### Conclusion

This experimental study has clearly demonstrated an experimental procedure for multi-phase fluid displacement

**Fig. 13**  $K_r$ - $S$  curve for water–diesel fuel pair (a) in drainage stage for  $S = 0.769$  (b) in imbibitions stage for  $S = 0.767$  (c) in drainage stage for  $S = 0.622$  (d) in imbibitions stage for  $S = 0.619$

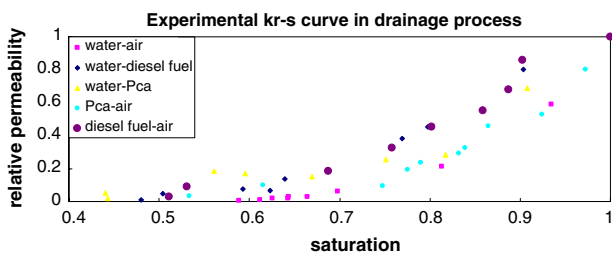
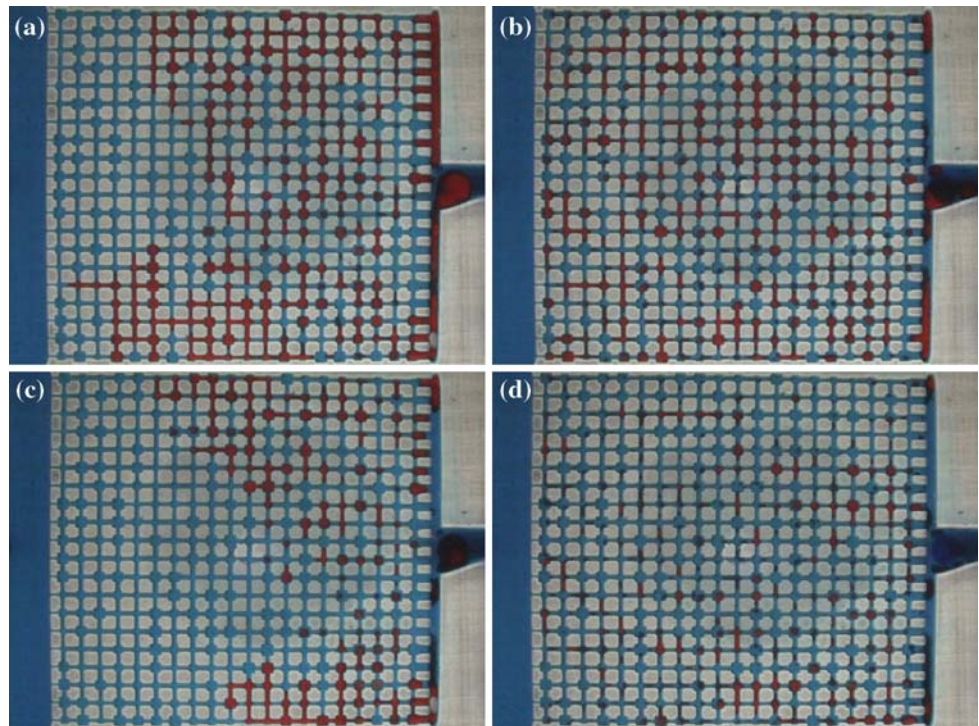


**Fig. 14** Experimental  $K_r$ - $S$  curve in drainage process for five fluid-pairs

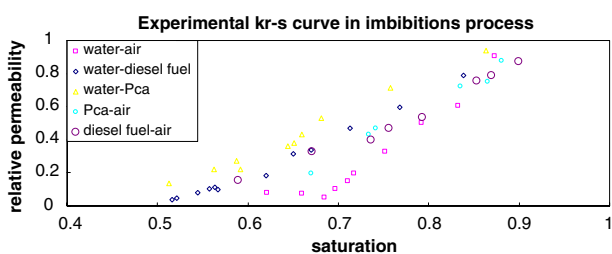


**Fig. 15** Experimental  $K_r$ - $S$  curve in imbibitions process for five fluid-pairs

on transparent micro-model and revealed qualitative interpretations on the fluid displacements related to the residual saturation of wetting fluid and the hysteresis relationship of relative permeability versus saturation. The experiments comprised complete displacement cycle of  $K_r$ - $S$ - $P$  including primary drainage and imbibition and the experimental results showed hysteresis phenomenon.

Although similar results have been found by other experimental researches, no previous studies have attempted to interpret the phenomenon. By examining the experimental images closely, the wetting phase fluid during the imbibition process distributed more uniformly than that in the drainage process for the same saturation. Hence, there were more micro channels connections in imbibition than that in drainage process, therefore, the imbibition process have higher relative permeability than the drainage process.

The results of the  $K_r$ - $S$  experiments for five fluid pairs also showed that the minimum saturation of wetting phase fluid (residual saturation) in which the system can maintain a flow under a reasonable hydraulic gradient decreased with the wettability increasing but increased with the interfacial tension increasing. Those interpretations and experimental results are valuable references for groundwater remediation and oil reservoir development. However, further research is still required to develop quantitative description for those phenomenons.

## References

- Al-Futaisi A, Patzek TW (2004) Secondary imbibition in NAPL-invaded mixed-wet sediments. *J Contam Hydrol* 74(1–4):61–81
- Ataie-Ashtiani B, Hassanizadeh SM, Oostrom M, Celia MA, White MD (2001) Effective parameters for two-phase flow in a porous medium with periodic heterogeneities. *J Contam Hydrol* 49:87–109
- Ataie-Ashtiani B, Hassanizadeh SM, Oostrom M, Celia MA, White MD (2002) Effects of heterogeneities on capillary pressure–

- saturation–relative permeability relationships. *J Contam Hydrol* 56:175–192
- Ataie-Ashtiani B, Hassanizadeh SM, Oung O, Weststrate FA, Bezuijen A (2003) Numerical modelling of two-phase flow in a geocentrifuge. *Environ Model Softw* 18:231–241
- Baker LE (1988) Three-phase relative permeability correlations. Society of Petroleum Engineers/Department of Energy Symposium on Enhanced Oil Recovery, Paper SPE 17369
- Bedient PB, Rifai HS, Newell CJ (1994) Ground water contamination: transport and remediation. Prentice-Hall, Englewood Cliffs
- Bradford SA, Leij FJ (1996) Predicting two- and three-fluid capillary pressure saturation relationships of porous media with fractional wettability. *Water Resour Res* 32(2):251–259
- Busby RD, Lenhard RJ, Rolston DE (1995) An investigation of saturation-capillary pressure relations in 2-fluid and 3-fluid systems for several NAPL in different porous-media. *Ground Water* 33(4):570–578
- Corapcioglu MY, Fedirchuk P (1999) Glass bead micro model study of solute transport. *J Contam Hydrol* 36:209–230
- Corapcioglu MY, Chowdhury S, Roosevelt SE (1997) Micro model visualization and quantification of solute transport in porous media. *Water Resour Res* 33:2547–2558
- Das DB, Hassanizadeh SM, Rotter BE, Ataie-Ashtiani B (2004) A numerical study of micro-heterogeneity effects on upscaled properties of two-phase flow in porous media. *Transp Porous Media* 56:329–350
- Das DB, Mirzaei M, Widdows N (2006) Non-uniqueness in capillary pressure–saturation–relative permeability relationships for two-phase flow in porous media: interplay between intensity and distribution of random micro-heterogeneities. *Chem Eng Sci* 61:6786–6803
- Demond AH, Roberts PV (1993) Estimation of two-phase relative permeability relationships for organic liquid contaminants. *Water Resour Res* 29:1081–1090
- Dullien FAL (1992) Porous media fluid transport and pore structure, 2nd edn. Academic Press, San Diego
- Fagerlund FF, Niemi A, Oden M (2006) Comparison of relative permeability–fluid saturation–capillary pressure relations in the modeling of non-aqueous phase liquid infiltration in variably saturated, layered media. *Adv Water Resour* 29:1705–1730
- Hassanizadeh SM, Celia MA, Dahle HK (2002a) Dynamic effect in the capillary pressure–saturation and its impact on unsaturated flow. *Vadose Zone Hydrol* 1:38–57
- Hassanizadeh SM, Celia MA, Dahle HK (2002b) Dynamic effect in the capillary pressure–saturation relationship and its impact on unsaturated flow. *Agric Sci* 7(2):69–71
- Helmig R (1997) Multiphase flow and transport processes in the subsurface. Springer, Berlin
- Hilfer R (2006) Capillary pressure, hysteresis and residual saturation in porous media. *Physica A* 359:119–128
- Jeong SW, Corapcioglu MY, Roosevelt SE (2000) Micro model study of surfactant foam remediation for residual trichloroethylene. *Environ Sci Technol* 34:3456–3461
- Jia C, Shing K, Yortsos YC (1999) Visualization and simulation of non-aqueous phase liquids solubilization in pore networks. *J Contam Hydrol* 35(4):363–387
- Kalaydjian FJ-M, Moulou J-C, Vizika O, Munkeerud PK (1997) Three-phase flow in water-wet porous media: gas/oil relative permeabilities for various spreading conditions. *J Petrol Sci Eng* 16:275–290
- Legait B (1983) Laminar flow of two phases through a capillary tube with variable square cross-section. *J Colloid Interface Sci* 96(1):28–38
- Lenormand R, Zarcone C, Sarr A (1983) Mechanisms of the displacement of one fluid by another in a network of capillary ducts. *J Fluid Mech* 135:337–353
- Leverett MC (1942) Capillary behavior in porous solids. *Trans AIME* 142:152–169
- Li K (2007) Scaling of spontaneous imbibition data with wettability included. *J Contam Hydrol* 89:218–230
- Li K, Horne RN (2004) An analytical scaling method for spontaneous imbibition in gas/water/rock systems. *SPE J* 9(3):322–329
- Muskat M, Meres MW (1936) The flow of heterogeneous fluids through porous media. *Physics* 7:346–363
- Oostrom M, Lenhard RJ (1998) Comparison of relative permeability–saturation–pressure parametric models for infiltration and redistribution of a light non-aqueous-phase liquid in sandy porous media. *Adv Water Resour* 21:145–157
- Parker JC, Lenhard RJ, Kuppasamy T (1987) A parametric model for constitutive properties governing multiphase flow in porous media. *Water Resour Res* 23(4):618–624
- Soll WE, Celia MA, Wilson JL (1993) Micro model studies of three-fluid porous media systems: pore-scale process relating to capillary pressure–saturation relationships. *Water Resour Res* 29(9):2963–2974
- Theodoropoulou MA, Karoutsos V, Kaspiris C, Tsakiroglou CD (2003) A new visualization technique for the study of solute dispersion in model porous media. *J Hydrol* 274:176–197
- Wessolek G, Plagge R, Leij FJ, van Genuchten MTh (1994) Analysing problems in describing field and laboratory measured soil hydraulic properties. *Geoderma* 64(1–2):93–110
- Van Dijke MIJ, Sorbie KS (2002) The relation between interfacial tensions and wettability in three-phase systems: consequences for pore occupancy and relative permeability. *J Petrol Sci Eng* 33:39–48
- Van Dijke MIJ, Sorbie KS (2007) Consistency of three-phase capillary entry pressures and pore phase occupancies. *Adv Water Resour* 30:182–198
- Van Dijke MIJ, Sorbie KS, McDougall SR (2001) Saturation-dependencies of three-phase relative permeabilities in mixed-wet and fractionally wet systems. *Adv Water Resour* 24(3):65–384